Proc. Natl. Acad. Sci. USA
Vol. 93, pp. 2370–2375, March 1996
Microbiology

Internal ribosomal entry site substitution eliminates neurovirulence in intergeneric poliovirus recombinants

(neuropathogenicity/attenuation)

MATTHIAS GROMEIER*, LOUIS ALEXANDER†, AND ECKARD WIMMER

Department of Molecular Genetics and Microbiology, State University of New York at Stony Brook, Stony Brook, NY 11794-5222

Communicated by Robert M. Chanock, National Institutes of Health, Bethesda, MD, October 19, 1995

ABSTRACT **Neuropathogenicity of poliovirus can be attenuated by mutations in the internal ribosomal entry site (IRES) within the 5′ nontranslated region of its genome. The Sabin vaccine strains used in prevention of poliomyelitis carry such mutations in their IRES elements. In addition, mutations within the structural and nonstructural proteins of Sabin strains may equally contribute to the attenuation phenotype. Despite their effectiveness as vaccines, the Sabin strains retain a neuropathogenic potential in animal models for poliomyelitis and, at a very low rate, they can cause poliomyelitis in vaccine recipients. The elimination of the neurocytopathic phenotype was achieved through the exchange of the entire poliovirus IRES with its counterpart from human rhinovirus type 2 without affecting growth properties in nonneuronal cells. The attenuating effect of the human rhinovirus type 2 IRES within the context of a poliovirus genome has been mapped to the 3′ portion of this genetic element.**

Models for the mechanism of eukaryotic translation demand ribosomal binding at a 5′ terminal cap and ribosome scanning until the proper site of initiation is recognized (1). However, efficient translation of picornavirus RNAs that lack a 5′ m^7GpppG cap structure (2) occurs via internal ribosomal entry within the 5′ nontranslated region (5′ NTR) (3–6). The presence of numerous clustered initiation codons with proper context for translational initiation within picornavirus 5′ NTRs makes a scanning mechanism implausible. It was found that disproportionally long picornavirus 5′ NTRs contain a cis-acting genetic element, the internal ribosomal entry site (IRES), that mediates internal ribosomal entry and cap-independent translational initiation (3–8). Trans-acting cellular and viral factors interacting with the IRES, which ensure proper initiation and stimulation of translation, have been identified (9–13). Although a large number of studies on IRES function (mostly in cell-free systems) have shed some light on the mechanism of translational initiation in IRES elements (reviewed in ref. 2), their function in determination of viral pathogenesis *in vivo* remains obscure.

We have constructed picornavirus genomic hybrids in which the IRES element of poliovirus (PV) was replaced with that of either encephalomyocarditis virus (EMCV) or human rhinovirus type 2 (HRV2). Exchange of its generic IRES element affected the most distinctive pathogenic property of PV. Neuropathogenicity in a mouse model for poliomyelitis was eliminated in viruses containing the HRV2 IRES while still present in attenuated PV vaccine strains currently in use. Recombinant PV strains featuring the HRV2 IRES regained neurovirulence upon transfer of two distinctive domains derived from the PV IRES. IRES-mediated cell specificity represents a new determinant of picornaviral pathogenesis at the level of viral gene expression.

The publication costs of this article were defrayed in part by page charge payment. This article must therefore be hereby marked "*advertisement*" in accordance with 18 U.S.C. §1734 solely to indicate this fact.

MATERIALS AND METHODS

Construction of Intergeneric PV Recombinants. The construction of PV1(ENPO) is described by Alexander *et al.* (14). PV1(ENPOS) was generated as follows: a fragment containing the EMCV IRES was PCR-amplified from PV1(ENPO) using primers a (5′-CCGTAACTTAGGAATTCC-3′) and b (5′-GCGGGTCGACCCACCATACGCTC-3′). A contiguous fragment encompassing the P1 region of PV1(S), encoding all PV1(S)-specific amino acid exchanges within the capsid, was PCR-amplified from a PV1(S) cDNA (kindly provided by A. Nomoto, Tokyo, Japan) using primers c (5′-GCGGGTCGAC-CATTAATTACACCACC-3′) and d (5′-TTTCTCGGGCAC-TGGAGCGC-3′). PV1(M) cDNA pPN6 (kindly provided by R. Andino, San Francisco) was cut with *Eco*RI and *Ava* I and ligated with both PCR fragments to yield PV1(ENPOS). PV1(RIPO) was constructed as follows: The HRV2 IRES was PCR-amplified from HRV2 cDNA (kindly provided by D. Blaas, Vienna, Austria) using primers e (5′-CCGAAT-TCAACTTAGAAGTTTTTCACAAAG-3′) and f (5′-CCTGAGCTCCCATGGTGCCAATATATATATTG-3′). An additional PCR fragment was amplified from pPN6 using primers g (5′-CCGAGCTCAGGTTTCATCACAG-3′) and h (5′-CCTGTGCTAGCGCTTTTTGCTC-3′) encoding the IRES-adjacent upstream region in P1. The PCR-amplified segments encompassing the HRV2 IRES and a fragment of P1 from the PV1(M) P1 region ligated to PV1 (ENPO), which was previously cut with *Eco*RI and *Nhe* I, yielded PV1(RIPO). PV1(RIPOS) was derived by PCR amplification of a P1 fragment from PV1(S) using primers g and h and subsequent ligation with the HRV2 IRES fragment obtained with primers e and f to PV1(ENPOS) previously cut with *Eco*RI and *Nhe* I. PV1(RNPL5) was constructed as follows: a fragment from the 5′ IRES (including domains I–IV) of HRV2 was PCR-amplified from HRV2 cDNA using primers e and i (5′-GGAGATCTCAAAGCGAGCACACGG-3′). A fragment from the 3′ IRES (including domains V and VI) was PCR-amplified from pPN6 using primers k (5′-GGAGATCTCCG-GCCCCTGAATGCGG-3′) and l (5′-CCTGAGCTCCCAT-TATGATACAATTGTCTG-3′). Both IRES fragments were ligated to PV1(RIPO) cut previously with *Eco*RI and *Sac* I. Each recombinant plasmid was linearized with *Sal* I and used as template for *in vitro* transcription. RNA produced from the templates was used to transfect HEp-2 cells by the DEAE transfection method. After occurrence of the cytopathic effect, virus was harvested from the transfected cells and propagated as described (15).

Abbreviations: 5′ NTR, 5′ nontranslated region; IRES, internal ribosomal entry site; PV, poliovirus; EMCV, encephalomyocarditis virus; HRV2, human rhinovirus type 2; wt, wild type; hPVR-tg mice, mice transgenic for human PV receptor; p.i., postinfection; pfu, plaque-forming units.

*To whom reprint requests should be addressed.
†Present address: Harvard Medical School, New England Regional Primate Research Center, Division of Microbiology, Southborough, MA 01772-9102.

Cell Lines and One-Step Growth Curves. Cell lines HEp-2, derived from a human laryngeal epidermoid carcinoma, and SK-N-MC, derived from a neuroblastoma in a human subject, were obtained from American type culture collection and grown in Dulbecco's minimal essential medium (DMEM; GIBCO), 10% fetal bovine serum (GIBCO), penicillin (100 units/ml), and streptomycin (100 μg/ml). HEp-2, SK-N-MC, and pSVLH20A (16) monolayers in 6-cm plastic culture dishes were inoculated with a viral suspension at a multiplicity of infection of 10 and gently shaken for 30 min at room temperature. Afterwards, the dishes were washed five times each with 5 ml of DMEM. Then the monolayers were overlaid with 2 ml of DMEM containing 2% fetal bovine serum. Synchronized infection was interrupted at the indicated intervals, cell monolayers were lysed by four consecutive freeze–thaw cycles, and the viral yield in the cell lysate was determined in a plaque assay.

RESULTS

Transposition of either the EMCV or the HRV2 IRES element into a PV type 1(Mahoney) [(PV1(M)] background resulted in viruses named PV1(ENPO) or PV1(RIPO), respectively. The plaque phenotypes with respect to PV1(M) were nearly identical [PV1(RIPO)] or reduced in size [PV1(ENPO)] (Fig. 1). To determine whether the species origin of the IRES influences cell type specificity of picornaviruses, growth kinetics of all constructs were determined in a neuroblastoma cell line of human origin (SK-N-MC) and compared with growth kinetics in HEp-2 cells, a human laryngeal epidermoid carcinoma cell line. HEp-2 cells were shown to be permissive for all three different IRES fragments yielding comparable amounts of viral progeny from each viral strain tested (Fig. 2*A*). Surprisingly, the study of growth kinetics of PV1(RIPO) in HEp-2 cells revealed an accelerated growth rate with respect to wild-type (wt) PV1(M), reaching optimal levels of viral yield ≈2 hr earlier than the latter (Fig. 2*A*).

Attenuated PV Sabin [PV(S)] vaccine strains with reduced neurovirulence exhibit impaired growth in SK-N-MC or SH-SY5Y neuroblastoma cells (18, 19). Dissection of the genotype of PV1(S) has revealed that a single point mutation at nucleotide 480 within the IRES of PV1(S) can compromise viral growth in a cell type-specific manner, resulting in a decreased ability of attenuated PV1(S) to replicate in cells of neuronal origin (2, 20).

The heterologous EMCV IRES element in PV1(ENPO) also significantly reduced replication of this strain in neuronal cells (Fig. 2*B*). Replacement of the PV IRES with that of HRV2, however, abrogated the ability of this strain [(PV1(RIPO)] to proliferate in SK-N-MC cells almost completely (Fig. 2*B*), whereas in HEp-2 cells it replicated at a rate exceeding that of PV1(M) (Fig. 2*A*).

Since we intended to use a murine model for assays of neurovirulence of the IRES recombinants (21–23), we had to exclude the possibility of IRES-dependent host restrictions. Both PV (24) and EMCV (25) are known to be neuropathogenic in mice but human rhinoviruses do not normally grow in cells of murine origin (26). However, the genetic locus of this restriction has been reported to map to the coding region of the nonstructural protein 2BC (26). In an effort to test whether the HRV2 IRES element can direct translational initiation in cells of murine origin, pSVLH20A, a murine fibroblast line constitutively expressing the α isoform of the human PV receptor

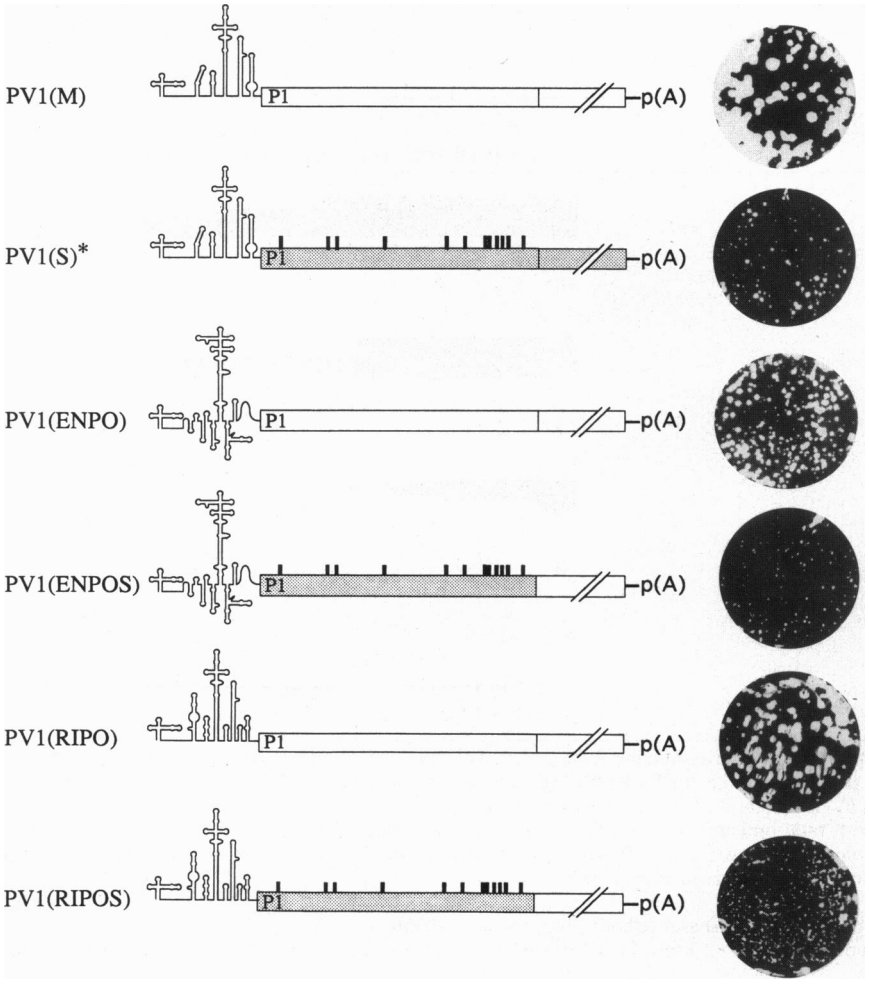

FIG. 1. Genetic structure and plaque phenotype of PV IRES recombinants. PV1(ENPO) and PV1(ENPOS) refer to hybrids containing the EMCV IRES. PV1(RIPO) and PV1(RIPOS) specify the HRV2 IRES. Reduction in plaque size seen with PV1(Sabin) [(PV1(S)] compared to its wt progenitor PV1(M) is reflected in the reduced plaque size of PV1(ENPOS) and PV1(RIPOS) with regard to their respective ancestors. Vertical bars indicate relative positions of amino acid exchanges within the PV1(S) capsid when compared to the PV1(M) sequence. *, The PV1(S) 5′ NTR contains seven point mutations with respect to PV1(M) that are not indicated (17).

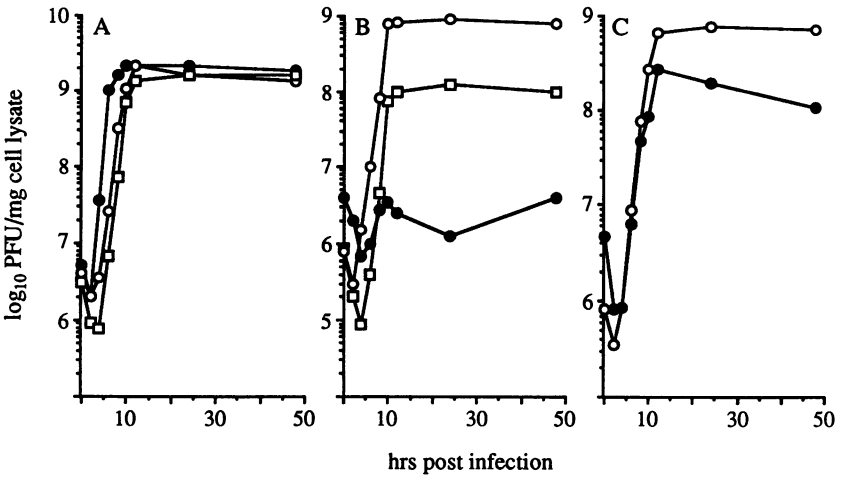

FIG. 2. Growth curves of PV1(M) (○), PV1(ENPO) (□), and PV1(RIPO) (●) in HEp-2 (*A*), SK-N-MC (*B*), and pSVLH20A cells (*C*). Synchronized infection of each cell type yielded viral offspring at different time intervals. Growth kinetics of PV1(RIPO) in comparison with PV1(M) showed accelerated dynamics in HEp-2 cells, virtually absent viral replication in SK-N-MC cells, and slightly reduced growth in murine pSVLH20A cells.

(16) was infected with PV1(RIPO). Infection of this murine cell line with PV1(RIPO) revealed efficient replication kinetics similar to that of PV1(M) except that the final yield was slightly lower than that of the wt virus. However, both PV1(M) and PV1(RIPO) showed delayed production of the final yield of progeny virus compared to growth kinetics in HEp-2 cells (compare Fig. 2 *A* and *C*).

All PV strains containing either the homologous or the heterologous IRES elements, were assayed to determine their neurovirulent potential in mice transgenic for the human PV receptor [hPVR-tg mice strain ICR.PVR.tgI (21)]. wt PV strains induce in these animals a neurological disease indistinguishable, clinically and histologically, from primate poliomyelitis (21–23, 27). hPVR-tg mice were infected by either the intravenous (i.v.) or the intracerebral (i.c.) route and the clinical course of ensuing neurological disease was monitored. Animal central nervous system tissues were analyzed histopathologically and assayed for viral replication. PV1(ENPO) had reduced neurovirulence when compared to PV1(M) (Table 1). Moreover, the injection of sublethal doses of PV1(ENPO) led to expression of a nonprogressive, incomplete paralytic disease (Fig. 3*C*), whereas neurological symptoms after inoculation of PV1(M) invariably progressed to fatality (Fig. 3*B*). Remarkably, PV1(RIPO) was devoid of any neuropathogenic potential and produced only a transient subtle paraparesis without positional abnormalities of the lower extremities (Fig. 3*A*, Table 1). PV recombinants containing the EMCV IRES element and the P1 capsid region of PV1(S) [see Fig. 1; PV1(ENPOS)] acquired the defective neuroinvasiveness phenotype of PV1(S). This was indicated by the need for

Table 1. Neurovirulence staging of PV recombinants in hPVR-tg mice

	LD_{50}, $\log_{10}$ pfu*		
	i.v.	i.c.	Intraspinal viral replication, $\log_{10}$ pfu per mg of tissue†‡
PV1(M)	4.1	2.2	
PV1(S)	—	6.3	ND
PV1(ENPO)§	6.8	4.8	
PV1(ENPOS)	—	7.0	ND
PV1(RIPO)¶	—	—	
PV1(RIPOS)	—	—	ND
PV1(RNPL5)	4.8	3.0	ND

0 1 2 3 4 5 6

Groups of four mice were infected with any given amount of virus ranging from 10^2 to 10^4 pfu i.c. and 10^3 to 10^5 pfu i.v. for PV1(M) and PV1(RNPL5); 10^5 to 10^8 pfu i.c. and i.v. for PV1(S), 10^3 to 10^7 pfu i.c. for PV1(ENPO), and 10^5 to 10^9 pfu i.v. for PV1(ENPO) and the remaining viruses by either route. LD_{50} values were calculated by the method of Reed and Muench (28).

*Negative sign indicates that poliomyelitic disease with fatal outcome was not observed after inoculation of 10^9 pfu.

†Virus titers were determined from homogenized spinal cord tissue from hPVR-tg mice infected with 5×10^5 pfu by the i.v. route. Each bar represents viral yield of a consecutive day p.i. starting with day 1 read from above.

‡ND, not done.

§Sublethal doses of this virus did cause incomplete poliomyelitic disease without progression to death.

¶A subtle transient paraparesis was observed after inoculation of $> 10^7$ pfu i.v. or 10^5 pfu i.c. Weakness was evident 18–24 hr p.i. and lasted for several days. There were no permanent deficiencies.

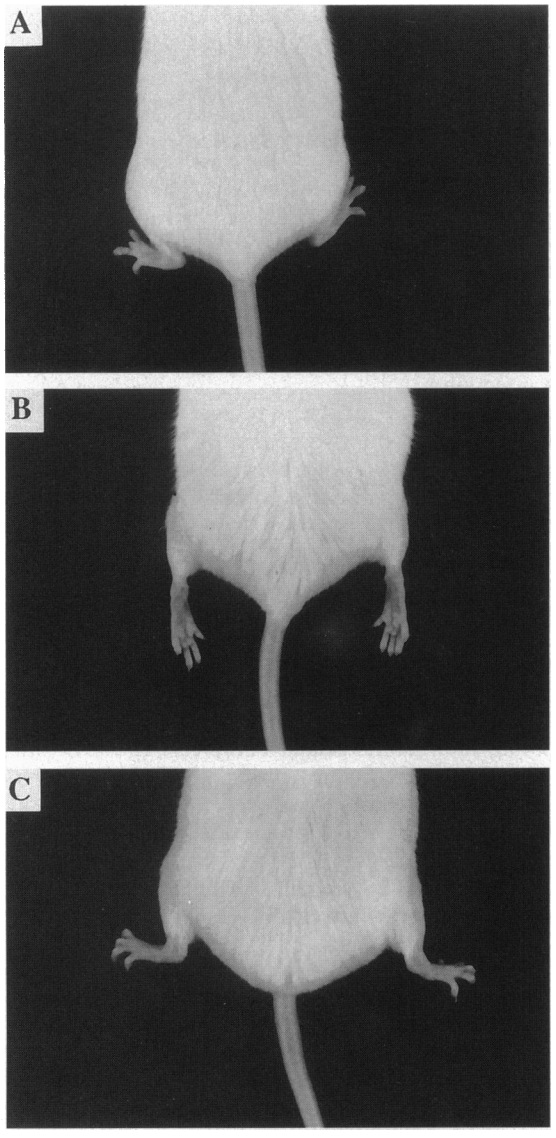

FIG. 3. Clinical appearance of hPVR-tg mice after infection with PV1(RIPO) (*A*), PV1(M) (*B*), and PV1(ENPO) (*C*). Symptomatic animals inoculated by either i.c. or i.v. injection with PV1(M) invariably developed flaccid paraparesis (*B*), which rapidly progressed to respiratory involvement. PV1(ENPO) in sublethal doses caused an aborted nonprogressive paralytic syndrome associated with pareses of the lower extremities, causing a characteristic abnormal posture of the lower body (*C*). Mice injected with PV1(RIPO) showed evidence of a transient weakness without positional abnormalities and only discrete loss of strength (*A*).

i.c. inoculation of PV1(ENPOS) to produce neurological symptoms (Table 1). Its counterpart containing the HRV2 IRES within a PV1(S) capsid [PV1(RIPOS)] was inert even after i.c. inoculation of massive virus titers.

Histopathological analysis revealed the pathological correlate of clinical findings in that different levels of viral neuropathogenicity were specific for each strain tested. While symptomatic infection with PV1(M) invariably resulted in eradication of the motoneuronal population within the spinal cord (Fig. 4*B*), the cord of animals infected with PV1(ENPO) at sublethal doses showed many intact motor neurons (Fig. 4*C*). i.c. injection with PV1(RIPO) did not cause any apparent alterations within the central nervous system (Fig. 4*A*). After administration of virus, spinal cord tissue was harvested from the mice at various stages. The tissue samples were then analyzed for the presence of viral particles (Table 1). PV1(M) and PV1(ENPO) replication within the spinal cord peaked at

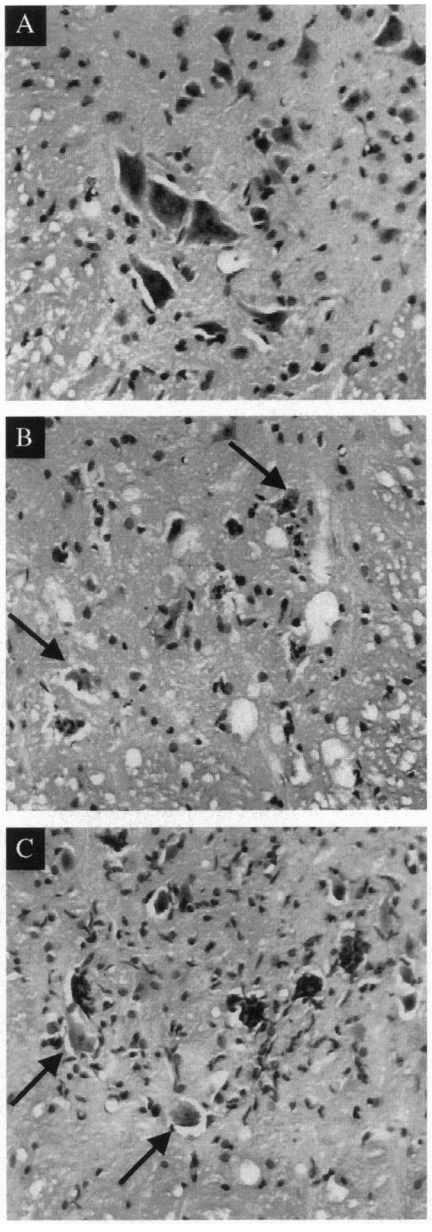

FIG. 4. Pathohistology of the anterior horn of the lumbar spinal cord after i.v. inoculation of 10^6 pfu of PV in hPVR-tg mice. (*A*) Inoculation of PV1(RIPO) never caused detectable pathological changes in areas of the central nervous system typically affected by PV. (*B*) After infection of mice with PV1(M), selective eradication of motor neurons within the anterior horn of the spinal cord, the hallmark of paralytic poliomyelitis, occurred. Remains of necrolytic motor neurons are indicated by arrows. Destruction of this group of neurons was always exclusive and complete. (*C*) In contrast, PV1(ENPO) replication within the spinal cord did leave numerous motor neurons unaffected (arrows), while others could be seen in different stages of cytopathic change. Histological procedures and neuropathogenicity staging are described (27). (×36.)

≈4 days postinfection (p.i.). PV1(ENPO), however, reproduced at a lower level (Table 1). At no time after i.c. inoculation of PV1(RIPO) was intraspinal replication evident with this variant (Table 1). It has been claimed previously that skeletal muscle can support PV replication in hPVR-tg mice (29). Quantification of viral progeny of PV1(RIPO) from skeletal muscle after intramuscular (i.m.) inoculation into the hamstring muscle revealed replication levels comparable to wt PV1(M) (Table 2).

We have tested whether injection of hPVR-tg mice with PV1(ENPO) [5×10^6 plaque-forming units (pfu)] or

Table 2. Replication of PV1(M) and PV1(RIPO) within skeletal muscle*

Virus inoculated	$\log_{10}$ pfu per mg of hamstring recovered on days p.i.			
	0	2	3	4
PV1(M) i.m.†	3.6	4.6	5.1	5.2
PV1(RIPO) i.m.	3.6	4.7	5.3	5.3
PV1(M) i.m. ntg‡	3.4	2.1	1.0	0
PV1(M) i.v.	2.6	2.9	3.1	3.1
PV1(RIPO) i.v.	2.5	3.2	3.3	3.4

*hPVR-tg mice or nontransgenic littermates were inoculated with 5×10^5 pfu of the respective virus strain via the i.v. route or into the right hamstring muscle (i.m.).
†hPVR-tg mice infected with 5×10^5 pfu of PV1(M) i.m. developed symptoms of poliomyelitis by day 4.
‡ntg, Nontransgenic littermates.

PV1(RIPO) (5×10^8 pfu) would confer protective immunity to PV. Accordingly, we challenged the animals 10 and 20 days after inoculation with PV1(ENPO) or PV1(RIPO) by i.v. infection with PV1(M) at amounts exceeding the i.v. LD_{50} dose 1000-fold. None of the animals of either group developed symptoms of poliomyelitis. Whether the protective effect was merely due to the injection of viral "antigen," or whether it required replication of the chimeric viruses is not known.

Since the determination of an attenuation phenotype of all three Sabin vaccine strains had been partially attributed to the presence of single mutations within domain V ("attenuation loop") of the PV IRES (2), we attempted to locate the IRES segment conferring a neurovirulent phenotype to PV1(M). Replacement of domains V and VI from the PV1(M) IRES in PV1(RIPO) yielded PV1(RNPL5) (Fig. 5), a viable virus with a plaque phenotype slightly larger than wt PV1(M) (data not shown). The composite IRES in PV1(RNPL5) restored a wt neurovirulent phenotype (Table 1). This observation confirms the major role of the 3′ part of the IRES in determination of a neurovirulent phenotype of PV.

DISCUSSION

Picornaviruses, a large family of human and animal pathogens, cause a bewildering array of disease syndromes, the molecular basis of which is poorly understood. The tropism of these viruses has been predominantly related to the cell-specific expression of their receptors (30). However, virion stability (as in the case of rhinoviruses) and cell-internal restriction of replication may play an equally important role in the outcome of an infection.

Although closely related with respect to virion structure and gene organization, the five genera of Picornaviridae can be roughly divided into two groups: entero-/rhinoviruses and cardio-/aphtho-/hepatoviruses (2). Correspondingly, picornavirus IRES elements have been divided into type 1 and type 2 elements on the basis of their sequence and structure similarities (2). In rapidly growing tissue culture cells such as HEp-2 cells, the two IRES types appear to function with similar efficiency (the IRES of hepatovirus being an exception). This is also apparent in the one-step growth curves of the intergeneric IRES hybrid viruses analyzed here (Fig. 2*A*). In cell-free systems, however, an IRES type-specific difference in promoting internal ribosomal entry can be clearly demonstrated (3). It has been speculated that this *in vitro* restriction of IRES function relates to deficiencies in the quality and/or amount of specific trans-acting factors (9–13). Generally, the efficiencies of translation covaried with the type of IRES element: type 1 IRES elements of entero- and rhinoviruses function poorly in rabbit reticulocyte lysates, whereas the type

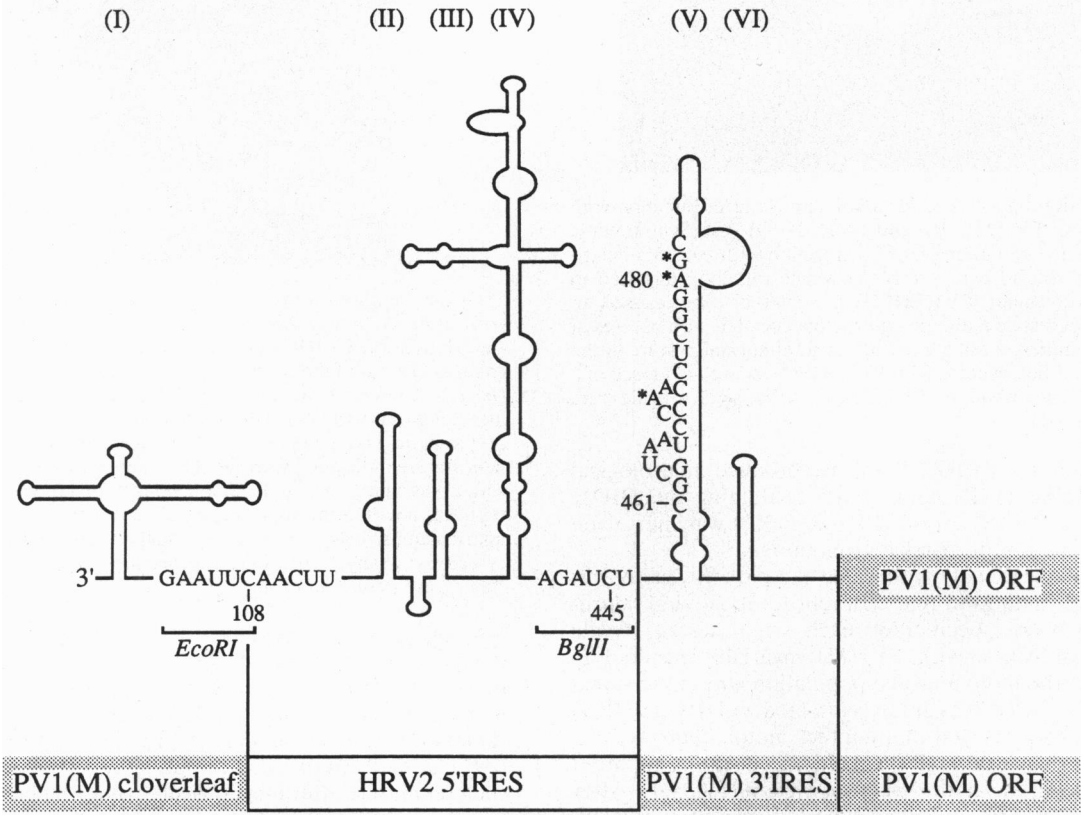

FIG. 5. Genetic structure of PV1(RNPL5). Map shows composition of a hybrid IRES element containing loops I, V, and VI of the PV1(M) IRES. Positions of individual attenuating mutations within all three Sabin vaccine strains are indicated by asterisks [nt 472, PV3(S); nt 480, PV1(S); nt 481, PV2(S); see ref. 2 for reference]. Roman numerals indicate distinct IRES domains.

2 IRESs of cardio- and aphthovirus are highly efficient in this system.

In view of these considerations, we were surprised to observe the extent of the limitation of PV1(RIPO) replication mediated by the HRV2 IRES in human neuroblastoma cells (Fig. 2*B*). The specific inactivity of the HRV2 IRES in neuronal cells was also borne out by the inability of PV1(RIPO) to cause poliomyelitis in hPVR-tg mice. A wt neurovirulent phenotype was restored by replacement of the IRES domains V and VI of HRV2 in PV1(RIPO) with their counterparts from PV1(M). The rescue of HRV2 IRES function in neurons through insertion of the PV1(M) domain V indicates the critical role of this structure in determination of a neurovirulent phenotype of PV.

The molecular basis of the functional restriction of the HRV2 IRES in tissue culture cells of neuronal origin remains to be determined. We have observed that intramuscular injection of hPVR-tg mice with PV1(RIPO) led to limited viral reproduction within the injected muscle at levels comparable to PV1(M). Unfortunately, the hPVR-tg mouse system is not a very useful animal model for studies of PV replication in the gastrointestinal tract because oral infection of these animals has been very difficult (22). Studies to determine the proliferation of PV1(RIPO) in monkeys remain to be done.

Global eradication of PV, targeted for the year 2000 (31) is being pursued with the use of the live, attenuated Sabin strains of PV (2). Although the Sabin vaccines cause, at a very low rate, poliomyelitis in vaccine recipients (32), it is unlikely that these agents will be replaced by other PV vaccine strains, derivatives of PV1(RIPO) included. However, our observation of the apparent specific activity of a picornavirus genetic element in expression of picornavirus polyproteins adds a new factor to the tissue tropism of picornaviruses in addition to the apparent distribution of cellular receptors (33–35) or factors that may modulate receptor function (36). The phenomenon of IRES-dependent restriction of viral gene expression in a tissue-specific manner may be exploited for rapid construction of vaccines against newly emerging viral pathogens or against already known viral agents. IRES-modulated expression of gene products may also facilitate the creation of expression vectors devoid of undesired pathogenic properties.

We thank A. Nomoto for generously providing hPVR-tg mice. This work was supported by National Institutes of Health Grants AI15122 and RO1AI32100, National Cancer Institute Grant CA28146, and the Human Frontiers Science Program Organization (RG 470/93-M). M.G. is supported by a fellowship from the Stipendienprogramm Infektionsforschung, Heidelberg, Germany.

1. Sonenberg, N. (1990) *Curr. Top. Microbiol. Immunol.* **161,** 23–47.
2. Wimmer, E., Hellen, C. U. T. & Cao, X. (1993) *Annu. Rev. Genet.* **27,** 353–436.
3. Jang, S. K., Kräusslich, H.-G., Nicklin, M. J. H., Duke, G. M., Palmenberg, A. C. & Wimmer, E. (1988) *J. Virol.* **62,** 2636–2643.
4. Jang, S. K., Davies, M. V., Kaufman, R. J. & Wimmer, E. (1989) *J. Virol.* **63,** 1651–1660.
5. Pelletier, J. & Sonenberg, N. (1989) *J. Virol.* **63,** 441–444.
6. Pelletier, J. & Sonenberg, N. (1988) *Nature (London)* **334,** 320–325.
7. Molla, A., Jang, S. K., Paul, A. V., Reuer, Q. & Wimmer, E. (1992) *Nature (London)* **356,** 255–257.
8. Jang, S. K., Pestova, T., Hellen, C. U. T., Witherell, G. W. & Wimmer, E. (1990) *Enzyme* **44,** 292–309.
9. Meerovitch, K., Svitkin, Y. V., Lee, H. S., Lejbkowicz, F., Kenan, D. J., Chan, E. K. L., Agol, V. I., Keene, J. D. & Sonenberg, N. (1993) *J. Virol.* **67,** 3798–3807.
10. Jang, S. K. & Wimmer, E. (1990) *Genes Dev.* **4,** 1560–1572.
11. Hellen, C. U. T., Witherell, G. W., Schmid, M., Shin, S. H., Pestova, T. V., Gil, A. & Wimmer, E. (1993) *Proc. Natl. Acad. Sci. USA* **90,** 7642–7646.
12. Hambidge, S. J. & Sarnow, P. (1992) *Proc. Natl. Acad. Sci. USA* **89,** 10272–10276.
13. Borman, A., Howell, M. T., Patton, J. G. & Jackson, R. J. (1993) *J. Gen. Virol.* **74,** 1775–1788.
14. Alexander, L., Lu, H.-H. & Wimmer, E. (1994) *Proc. Natl. Acad. Sci. USA* **91,** 1406–1410.
15. Lu, H.-H., Yang, C.-F., Murdin, A. D., Klein, M. H., Harber, J. J., Kew, O. M. & Wimmer, E. (1994) *J. Virol.* **68,** 7507–7515.
16. Mendelsohn, C. L., Wimmer, E. & Racaniello, V. R. (1989) *Cell* **56,** 855–865.
17. Nomoto, A., Omata, T., Toyoda, H., Kuge, W., Horie, H., Kataoka, Y., Genba, Y., Nakano, Y. & Imura, N. (1982) *Proc. Natl. Acad. Sci. USA* **79,** 5793–5797.
18. Agol, V. I., Drozdov, S. G., Ivannikova, T. A., Kolesnikova, M. S., Korolev, M. B. & Tolskaya, E. A. (1989) *J. Virol.* **63,** 4034–4038.
19. LaMonica, N. & Racaniello, V. R. (1989) *J. Virol.* **63,** 2357–2360.
20. Omata, T., Kohara, M., Abe, S., Itoh, H. Komatsu, T., Arita, M., Semler, B. L., Wimmer, E., Kuge, S., Kameda, A. & Nomoto, A. (1985) in *Vaccines 85: Molecular and Chemical Basis of Resistance to Parasitic, Bacterial, and Viral Diseases*, eds. Lerner, R. A., Chanock, R. M. & Brown, F. (Cold Spring Harbor Lab. Press, Plainview, NY), pp. 279–283.
21. Koike, S., Taya, C., Kurata, T., Abe, S., Ise, I., Yonekawa, H. & Nomoto, A. (1991) *Proc. Natl. Acad. Sci. USA* **88,** 951–955.
22. Horie, H., Koike, S., Kurata, T., Sato-Yoshida, Y., Ise, I., Ota, Y., Abe, S., Hioki, K., Kato, H., Taya, C., Nomura, T., Hashizume, S., Yonekawa, H. & Nomoto, A. (1994) *J. Virol.* **68,** 681–688.
23. Ren, R., Costantini, F., Gorgacz, E. J., Lee, J. J. & Racaniello, V. R. (1990) *Cell* **63,** 353–362.
24. Armstrong, C. (1939) *Public Health Rep.* **54,** 2302–2305.
25. Hahn, H. & Palmenberg, A. C. (1995) *J. Virol.* **69,** 2697–2699.
26. Yin, F. H. & Lomax, N. B. (1983) *J. Virol.* **48,** 410–419.
27. Gromeier, M., Lu, H.-H. & Wimmer, E. (1995) *Microb. Pathog.* **18,** 253–262.
28. Reed, L. J. & Muench, H. (1938) *Am. J. Hyg.* **27,** 493–495.
29. Ren, R. & Racaniello, V. R. (1992) *J. Virol.* **66,** 296–304.
30. Wimmer, E., Harber, J. J., Bibb, J. A., Gromeier, M., Lu, H.-H. & Bernhardt, G. (1994) in *Cellular Receptors for Animal Viruses*, ed. Wimmer, E. (Cold Spring Harbor Lab. Press, Plainview, NY), pp. 101–128.
31. Expanded Programme on Immunization (1989) *Global Poliomyelitis Eradication by the Year 2000: Manual for Managers of Immunization Programmes on Activities Related to Polio Eradication* (World Health Organ., Geneva), pp. 35–64.
32. Sutter, R. W., Patriarca, P. A., Brogan, S., Malankar, P. G., Pallansch, M. A., Kew, O. M., Bass, A. G., Cochi, S. L., Alexander, J. P., Hall, D. B., Suleiman, A. J. M., Alghassany, A. A. K. & Elbualy, M. S. (1991) *Lancet* **338,** 715–720.
33. Freistadt, M. (1994) in *Cellular Receptors for Animal Viruses*, ed. Wimmer, E. (Cold Spring Harbor Lab. Press, Plainview, NY), pp. 445–461.
34. Crowell, R. L. & Tomko, R. P. (1994) in *Cellular Receptors for Animal Viruses*, ed. Wimmer, E. (Cold Spring Harbor Lab. Press, Plainview, NY), pp. 75–99.
35. Koike, S., Aoki, J. & Nomoto, A. (1994) in *Cellular Receptors for Animal Viruses*, ed. Wimmer, E. (Cold Spring Harbor Lab. Press, Plainview, NY), pp. 463–480.
36. Shepley, M. P. (1994) in *Cellular Receptors for Animal Viruses*, ed. Wimmer, E. (Cold Spring Harbor Lab. Press, Plainview, NY), pp. 481–491.